



OPEN

SUBJECT AREAS:
SPINTRONICS
MAGNETIC PROPERTIES AND
MATERIALS
APPLIED PHYSICSReceived
5 March 2014Accepted
4 August 2014Published
21 August 2014Correspondence and
requests for materials
should be addressed to
Z.D.Z. (zdzhang@imr.
ac.cn) or T.Y.
(yangteng@imr.ac.cn)

Flower-like dynamics of coupled Skyrmions with dual resonant modes by a single-frequency microwave magnetic field

Yingying Dai, Han Wang, Teng Yang, Weijun Ren & Zhidong Zhang

Shenyang National Laboratory for Materials Science, Institute of Metal Research, Chinese Academy of Sciences, 72 Wenhua Road, Shenyang, 110016, P. R. China.

Resonant excitations of confined systems have aroused much attention because of their potential application in future microwave devices and spintronics. Under resonant excitations, the motion of topological objects exhibits circular, elliptical or even stadium-like dynamics. However, more complex non-linear resonant excitations of topological objects in confined systems have seldom been reported and the associated physical mechanism remains unclear. Here, we present an observation of flower-like resonant excitations for coupled skyrmions in Co/Ru/Co nanodisks activated by a single-frequency microwave magnetic field by means of numerical simulation. We find that flower-like dynamics of coupled skyrmions is always accompanied by an excitation of an eigenfrequency near 1.15 GHz, which is strongly associated with the large non-local deformation of the topological density distribution of coupled skyrmions. These results distinguish a skyrmion from other topological objects in dynamics and will be instrumental to the manipulation of skyrmions for applications.

Since proposed by Skyrme to explain hadrons in nuclear physics¹, skyrmions have been attracting considerable academic and technical interest because skyrmion presents transport properties associated with its global smooth topological spin texture^{2–8}. Magnetic skyrmion and skyrmion crystal have recently been observed experimentally in chiral magnets^{9–13}, and have also been predicted to exist in coupled ordinary nanomagnets^{14,15}. Furthermore, promising potential applications are envisioned for skyrmions in next-generation high-density storage and future microwave devices^{16,17} because of their small size of 10–100 nm and special topological nature. Considering the practical applications, the search for methods of manipulating skyrmions that are embedded in magnetic conductors or insulators (such as Cu₂OSeO₃) and the investigation of skyrmion dynamics are issues of vital importance. Spin-polarized current has been extensively used to drive skyrmions in conductors^{3,8}, but manipulation of skyrmions with a microwave field or a thermal current is still an important challenge^{18,19}. Skyrmion dynamics under a microwave field presents various resonant spin-wave modes with small amplitudes and an alluring nonreciprocal transport effect^{2,20}. However, resonant excitation behavior of skyrmions in a microwave field has seldom been reported and investigating the nonlinear resonant excitation is helpful for understanding the dynamics of the skyrmion. Unlike a vortex with local deformation at the core and a bubble with local deformation at the domain wall^{21–23}, a skyrmion moves with large non-local deformation. Based on its non-local deformation, the mechanisms of its dynamics are far from clear. Questions are what is the relationship between variation of deformation and trajectory of excitation, how can one control a skyrmion by resonance, etc.

Here we report the first observation of flower-like resonant trajectories in Co/Ru/Co nanodisks under a single-frequency microwave magnetic field by means of micromagnetic simulations. The origin of the observed non-linear dynamics is interpreted as a combination of the large non-local deformation of the topological density distribution arising from the global smooth spin texture and the coupling of the resonant modes in coupled skyrmions. We find that the resonant excitations are controllable by tuning the frequency and the amplitude of the microwave field to adjust the deformation of the topological density distribution. The present work unveils the importance of the non-local nature of the topological density distribution for the skyrmion dynamics and the prospects of skyrmions for spintronic applications.



Results

A skyrmion is a nontrivial topological object with stable spin swirl and integer skyrmion number (topological charge) defined by the following formula^{12,24}:

$$Q = \frac{1}{4\pi} \iint q dx dy, \quad q \equiv \mathbf{m} \cdot (\partial_x \mathbf{m} \times \partial_y \mathbf{m}), \quad (1)$$

where q is the topological density and \mathbf{m} the unit vector of the local magnetization. Coupled skyrmions with opposite chiralities have been obtained in a Co/Ru/Co nanodisk without taking into account the Dzyaloshinsky-Moriya interaction (DMI), as shown in Fig. 1a. The topological charge of every skyrmion is minus one due to the same polarity. Figure 1b presents the topological density distribution of a static skyrmion in the top nanolayer with a radial symmetry distribution. This global distribution is different from those of other

topological objects (such as Vortex, Meron and Bubble shown in Supplementary Fig. S1). In the center of the skyrmion, $|q|$ has the highest value. From the center to periphery, $|q|$ firstly decreases from 8.8×10^{-4} to $3.2 \times 10^{-4} \text{ nm}^{-2}$, then increases to a local maximum near the skyrmion radius and finally gradually decreases to $0.4 \times 10^{-4} \text{ nm}^{-2}$ at the boundary ($|q|$ as function of the radius is given in Supplementary Fig. S2).

We investigate the resonant excitation behavior of coupled skyrmions by applying a microwave magnetic field along the $+x$ direction on the top nanolayer, as shown in Fig. 1b. If one of the coupled skyrmions is moved from its central equilibrium position by the torque of the external field, the other one is stimulated by the strong magnetostatic coupling and a non-local deformation of the topological density distribution is created¹⁴ (as will be shown later). Consequently, the trajectory of the skyrmion core becomes complicated and sometimes it is tricky to identify the exact core position. We have used the guiding center (R_x, R_y) of the skyrmion (the center of topological charge) to determine the skyrmion center position and the radius of the skyrmion motion. The guiding center is defined by²⁵:

$$R_x = \frac{\iint x q dx dy}{\iint q dx dy}, \quad R_y = \frac{\iint y q dx dy}{\iint q dx dy}, \quad (2)$$

where q is the topological density defined in Eq. (1). Figure 1c shows the maximum steady-orbit radius R , which the guiding center can reach, as a function of the microwave frequency. The amplitude of the microwave magnetic field is set to be 100 Oe, except for the three points marked by blue stars where 50 Oe is used because of the appearance of a very strong resonance. In the microwave field, the guiding center of the skyrmion rotates around the nanodisk center and two resonance excitation modes are observed: mode 1 for clockwise (CW) rotation of guiding center in the low-frequency region and mode 2 for counterclockwise (CCW) rotation in the high-frequency region, both of which are coupled with each other²⁶. The two modes with opposite rotation direction are analytic solutions of the generalized Thiele's equation. The forms of the solutions are²³:

$$\omega_{\pm} = -G/2M \pm \sqrt{(G/2M)^2 + K/M}, \quad (3)$$

where G is the gyrocoupling vector, M the effective mass and K the stiffness coefficient. Equation (3) indicates that the high-frequency mode 2 is more sensitive to mass change than the low-frequency mode 1, which results in a much wider frequency range for mode 2 than for mode 1, so that the frequency for mode flipping is close to the low-frequency mode (around 2 GHz). Furthermore, in the Supplementary Fig. S6 the dependence of R on the field amplitude is also given. The frequency of the field is chosen to be 1.00 GHz, which activates linear dynamics: the plot of R as a function of the field amplitude shows an almost linear relationship.

From the gyrotropic motion of the guiding center, we can obtain the eigenfrequencies of the coupled skyrmion, as demonstrated in Ref. 14. First, a square-wave pulsed magnetic field with 10-ns width and 50-mT magnitude is applied to the top nanolayer to shift the guiding center over some distance and then, after the field is switched off, the guiding center will gyrate around the center of the nanodisk. Eigenfrequencies of near 1.15 GHz (for a circular trajectory), and 1.00 and 5.00 GHz (for a hexagonal trajectory) are obtained by means of the fast Fourier transform (FFT) spectrum of the trajectory of gyration. Figure 1c shows two pronounced peaks of R : one at 1.13 GHz in the region of mode 1 and the other at 4.75 GHz in the region of mode 2. The asymmetry of the first peak may have by two origins: 1) the field amplitude used for the three star points is smaller than that for the other points; 2) the superposition of the two peaks with eigenfrequencies 1.00 and 1.15 GHz. The frequency of 1.13 GHz of the first peak corresponds to the eigenfrequency of the circular trajectory. The frequency range of 4.60 ~ 4.85 GHz of the second peak, where a complicated dynamical behavior is found as

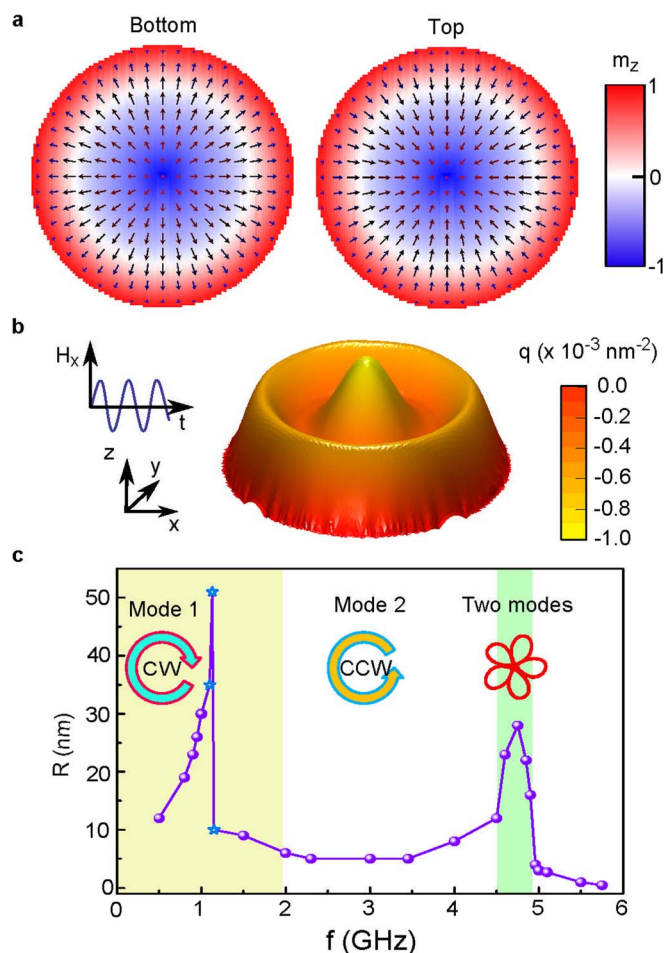


Figure 1 | Sketch of the topological density distribution and two excitation modes of skyrmion dynamics. (a) Magnetization distribution in the top and the bottom nanolayers. The colors represent the magnitude of the out-of-plane magnetization component (m_z) and the arrows indicate the direction of the in-plane magnetization component at every point. (b) The topological density distribution of a static skyrmion in the top nanolayer of a Co/Ru/Co nanodisk. q is the topological density. (c) Frequency dependence of the maximal radius R at which the guiding center can reach when skyrmion is excited by a microwave magnetic field. The field amplitude is set to be 100 Oe, except for the three points indicated by blue stars where 50 Oe is used because of the appearance of a very strong resonance. The excitation mode is clock-wise for field frequencies below 2.00 GHz (in the yellow region), and counterclock-wise above 2.00 GHz. In the green region, two modes with opposite rotation directions coexist.



shown in Fig. 2, seems to deviate from the eigenfrequency of 5.00 GHz for the hexagonal trajectory. Actually, the resonance peak at 5.00 GHz still exists, which indirectly may be concluded from the decreasing amplitude with increasing frequency which starts from 5.00 GHz. This peak is more or less hidden behind a pronounced peak around 4.60 GHz. This frequency is an overtone of 1.15 GHz and activates the base mode, thereby giving rise to two excitation modes and a large amplitude. In the frequency range 4.60 ~ 4.85 GHz, the rotation direction of the guiding center is initially CCW and becomes CW for steady orbits. The physical mechanism behind this novel non-linear dynamics and the appearance of the second peak needs further investigation.

Now, we focus on the interesting frequency range 4.50 ~ 4.85 GHz. The corresponding trajectories of coupled skyrmions due to resonant excitations are shown in Fig. 2. In a microwave field, the guiding center firstly rotates around the nanodisk center with an increasing radius until it reaches its steady orbits with periodic behavior (Fig. 2a). On the other hand, for quasi-periodic behavior, trajectories with the same radius have phase differences between different periods (Fig. 2b–2d). To illustrate the different results clearly, only the steady parts of trajectories are shown in the range of 30 ~ 50 ns. A steady orbit in a field with frequency of 4.50 GHz is circular with a radius of 12 nm, which is commonly observed in the dynamics of vortices and skyrmions excited by an alternating magnetic field. However, when the field frequency is between 4.60 GHz and 4.85 GHz, the steady orbit transforms to a flower-like orbit with increased amplitude, which is quite unusual. The one-period trajectories presented in the insets at the lower-right corners of Figs. 2b–d show five “petals”. These petals evolve with time into ribbon- or flower-like trajectories with quasi-periodicity due to a phase difference between the different periods. In addition, the phase shift increases from 0.02 to 0.15 radian if the frequency of the magnetic field changes from 4.60 to 4.85 GHz. The flower-like dynamics may be observed indirectly in an experiment: By using Lorentz transmis-

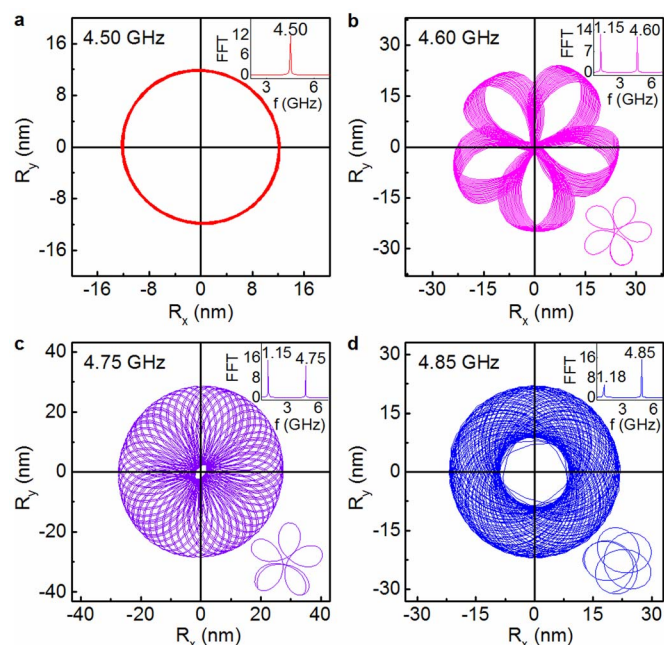


Figure 2 | Topological excitations of a skyrmion by microwave fields with different frequencies. Trajectories of the guiding center (R_x , R_y) of a skyrmion in the top nanolayer in 30 ~ 50 ns for frequencies of the microwave field of 4.50 (a), 4.60 (b), 4.75 (c) and 4.85 (d) GHz. The amplitude of the field is 100 Oe. The insets in the upper- and lower-right corners show the corresponding FFT spectra and the corresponding trajectories in about one period, respectively.

sion electron microscopy (LTEM)^{10,27} to obtain the magnetization distribution at different times and then calculating the position of the guiding center by means of Eq. (2). The FFT spectra of the trajectories are shown in the insets at the upper-right corners of Fig. 2a–d. During the steady-motion time (30–50 ns), the FFT spectra do not change with the length of time. Only one resonant frequency is observed in the circular trajectory excited by a field of frequency 4.50 GHz, whereas in a field of other frequency, an additional frequency around 1.15 GHz, which is reminiscent of the eigenfrequency of 1.15 GHz, shows up. The FFT intensity of the intrinsic mode and the intensity ratio between the two modes change with frequency.

To understand the flower-like trajectories better, a microwave field is applied to activate the topological excitation of the coupled skyrmion with a fixed frequency of 4.60 GHz but with amplitude varying from 20 to 500 Oe. The results are presented in Fig. 3. Surprisingly, when field amplitude is 20 Oe, the trajectory with a small radius of less than 2 nm is a circle instead of flower-like (Fig. 3a). The corresponding FFT spectrum shows only one peak at 4.60 GHz. As the amplitude increases, the maximum radius increases, and trajectory changes to flower-like. With further increasing amplitude from 60 Oe to 140 Oe, the flower-like trajectory changes from a sunflower to a bauhinia, due to a reduced phase shift from 0.18 to 0.01 radian. As field amplitude reaches 500 Oe, the trajectory becomes quite distinct from the previous ones, with six “petals”, instead of five, in each period (Fig. 3d). The corresponding FFT spectra in Figs. 3b–d are shown in the insets. Besides the peak at 4.60 GHz, associated with the external field, another peak near 1.15 GHz expectedly appears again. With increasing field amplitude, the intensity of peak at this frequency first increases and reaches its maximum at 100 Oe. Then the intensity decreases again with further increasing field amplitude, resulting in a decreased phase shift and different flower-like trajectories. It should be noted that, when the field amplitude is as large as 500 Oe, many frequencies apart from 1.15 and 4.60 GHz appear, which accounts for the six “petals” of the trajectory.

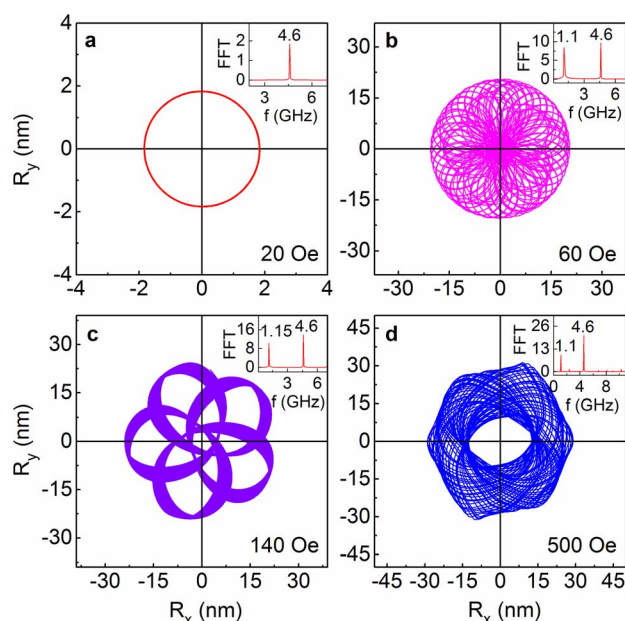


Figure 3 | Influence of the amplitude of a microwave field on the trajectory of the guiding center. The frequency of the microwave field is 4.60 GHz. (a), (b), (c) and (d) show the trajectories of the guiding center in 30 ~ 50 ns when the skyrmion is excited by a field of 20, 60, 140 and 500 Oe, respectively. The insets in the upper-right corners show the corresponding FFT spectra.



Figures 2 and 3 demonstrate that the flower-like trajectories are associated with an excitation of an intrinsic mode near 1.15 GHz, and the variation of the FFT intensity with the field amplitude at this eigenfrequency leads to different trajectories. To understand why the 1.15 GHz mode can be excited and exist stably in a microwave field of 4.60 ~ 4.85 GHz, Fig. 4 shows the topological density distribution of skyrmions corresponding to a maximum deformation in Fig. 3. The topological distribution of a static skyrmion has radial symmetry which, however, is broken as the skyrmion is activated by a microwave magnetic field. The deformation of the topological density distribution increases with field amplitude, becomes global if the amplitude larger than 20 Oe, and the topological density distribution becomes very complex when the field is as large as 450 Oe. To quantify the level of deformation, we start from Eq. (1) to calculate time-dependent value of the topological density change in a field as follows:

$$D = \iint |q(t) - q(0)| dx dy. \quad (4)$$

Figure 5a shows the time dependence of D in the dynamical process of a skyrmion in a microwave field (4.60 GHz and 100 Oe). D varies periodically between 6.1 and 2.6, in a similar manner as the trajectory of the guiding center in Fig. 2b, which implies a strong correlation between the topological density distribution and the non-linear dynamics of the skyrmion. Similar to the trajectory of the guiding center, also D is depending on the field amplitude. Figure 5b shows the field dependence of the average D (filled dots) and the oscillation of D (vertical bars) in one period during steady excitation. D is less than 0.5 at 20 Oe and initially increases monotonously to 4.50 at 100 Oe. As the amplitude further increases, D starts to decrease till 200 Oe and then increases again almost linearly to the highest value of 10.1.

To unveil the role played by the energy terms behind the flower-like trajectory, we also show in Figs. 5c and 5d the energy variations corresponding to the D variation in Figs. 5a and 5b. To note here that all energy terms vary periodically with time but only energies that contribute dominantly to the total energy are shown in Figs. 5c and 5d. The uniaxial anisotropy energy (E_{an}) and the demagnetization energy (E_{dem}) vary oppositely to each other with time and both of them are found to play a major role since the variation range of both

the E_{an} and E_{dem} is one order of magnitude as large as that of the total energy (E_{tot}). More importantly is the field dependence of the energy terms, which is similar to that of D . Figure 5d shows the field dependence of the average E_{tot} , E_{an} , E_{dem} (filled dots) and the E_{tot} oscillation (vertical bars) in one period during steady excitation. The E_{tot} oscillation, which shows the competition between sub-energy terms, exhibits a very similar behavior to the oscillation of D , suggesting a connection between D and competition among sub-energy terms. Moreover, the curves of E_{tot} and E_{an} agree well with that of D but with E_{an} varying faster than E_{tot} whereas E_{dem} has an opposite variation, all of which indicate that the competition existing between the E_{an} and E_{dem} leads to the variation of D and, thus, to the flower-like dynamics.

To clarify some possible issues such as whether the dynamics of a skyrmion in a microwave field can be simply depicted by the skyrmion core displacement ($m_z = -1$), we show in Fig. 6 the deformation of magnetization distribution which corresponds to the topological density distribution of skyrmion in Fig. 4. From Fig. 6a, not only the core displacement ($m_z = -1$) but also the boundary deformation ($m_z = 0$) is observed in the magnetization distribution. As the field amplitude increases, both the core displacement and the boundary deformation become larger. To quantify such deformations, we show in Fig. 6b the maximum position displacement from the zero-field position of m_z (equals to -1 and 0) as a function of the field amplitude. The displacement of core at $m_z = -1$ increases initially to 18 nm and drops to 2 nm, and then rises again to 20 nm, which has a variation similar to D , whereas the displacement of the boundary at $m_z = 0$ increases all the way from 0 to 17 nm as the field amplitude increases. It is interesting to see that, although the displacement of skyrmion core as a function of field amplitude is similar to that of the topological density distribution, the boundary deformation also has to be taken into account. Obviously, the dynamics of a skyrmion in a microwave field is more complex than that of a vortex and cannot simply be depicted by the motion of the skyrmion core ($m_z = -1$).

Figures 3–5 imply that it is the deformation of the topological density distribution that gives rise to the stable existence of the mode near 1.15 GHz and thus leads to the flower-like trajectories. Nevertheless, it is still unclear how deformation of the distribution leads to the stable existence of mode 1. To elucidate the role of the

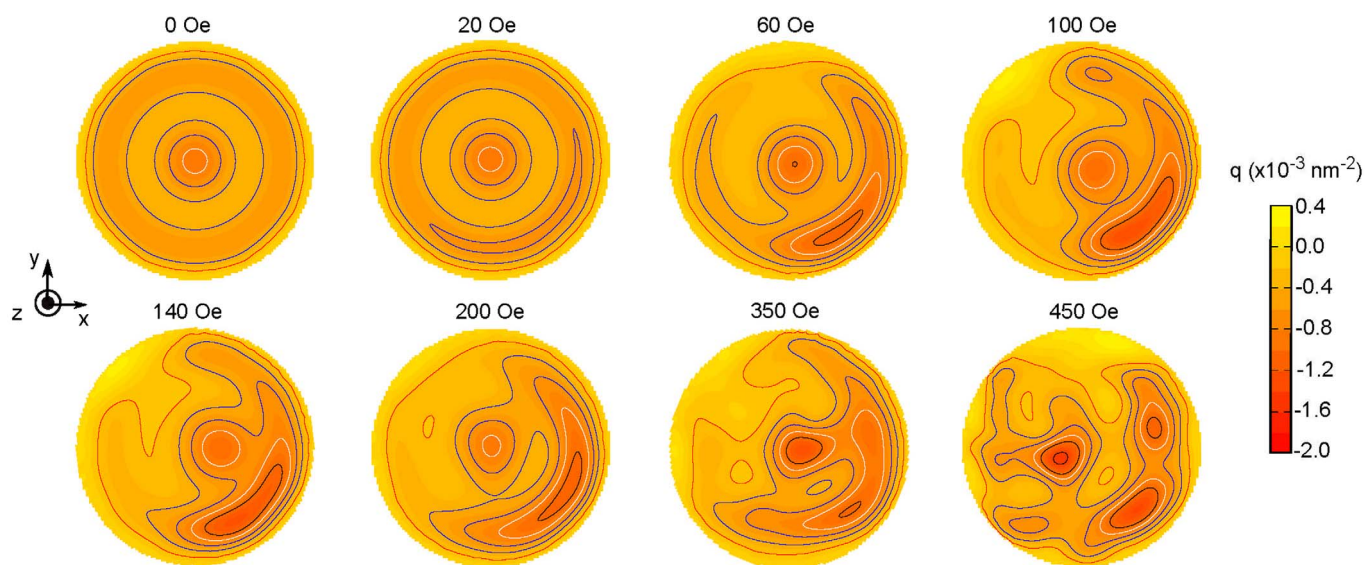


Figure 4 | The topological density distribution of skyrmion in different microwave fields. The frequency of the microwave field is 4.60 GHz and the amplitudes are in the range 0 ~ 450 Oe. The figure shows the distribution at the time that D is maximal in one period. To compare the results easier, the distribution has been rotated by hand. The topological density distribution has radial symmetry without applied field and with increasing field amplitude, the deformation of the distribution increases and large non-local deformation takes place.

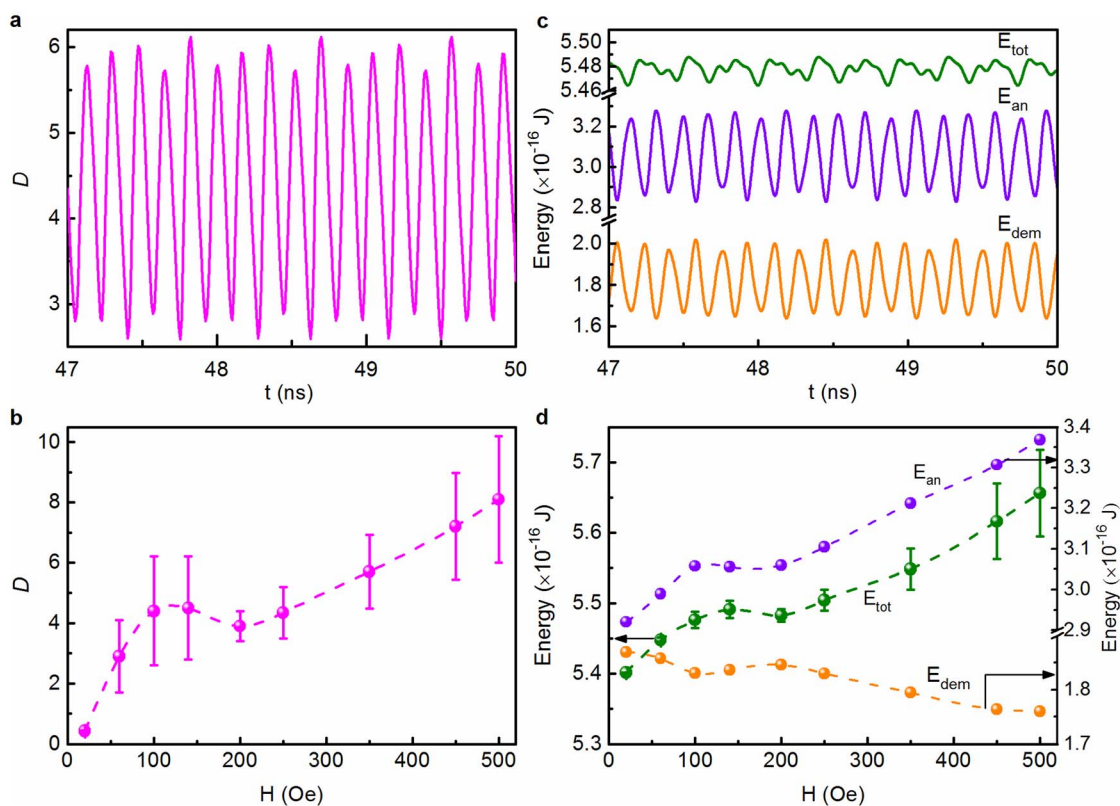


Figure 5 | Deformation of the topological density distribution and the corresponding variation of energy. Time dependence of (a) D and (c) the corresponding energies for a steady skyrmion trajectory excited by a microwave field of frequency 4.60 GHz and amplitude 100 Oe. The average and the variation of (b) D and (d) the corresponding energies as a function of field amplitude in the range 20 ~ 500 Oe. Average values are indicated by filled dots and the variation by bars. Only the energies (uniaxial anisotropy energy E_{an} and demagnetization energy E_{dem}) which contribute dominantly to the total energy E_{tot} are shown here. Only the variation of E_{tot} is shown in (d).

deformation of the topological density distribution, it is demonstrated in Fig. 7 that the flower-like trajectory can be tuned by controlling the level of deformation even at a frequency far from the two

eigenfrequencies (1.15 and 5.00 GHz)¹⁴. The frequency of 3.45 GHz is chosen. The trajectory is approximately circular for the small field amplitude 100 Oe and, as shown in Fig. 7a, the corresponding FFT

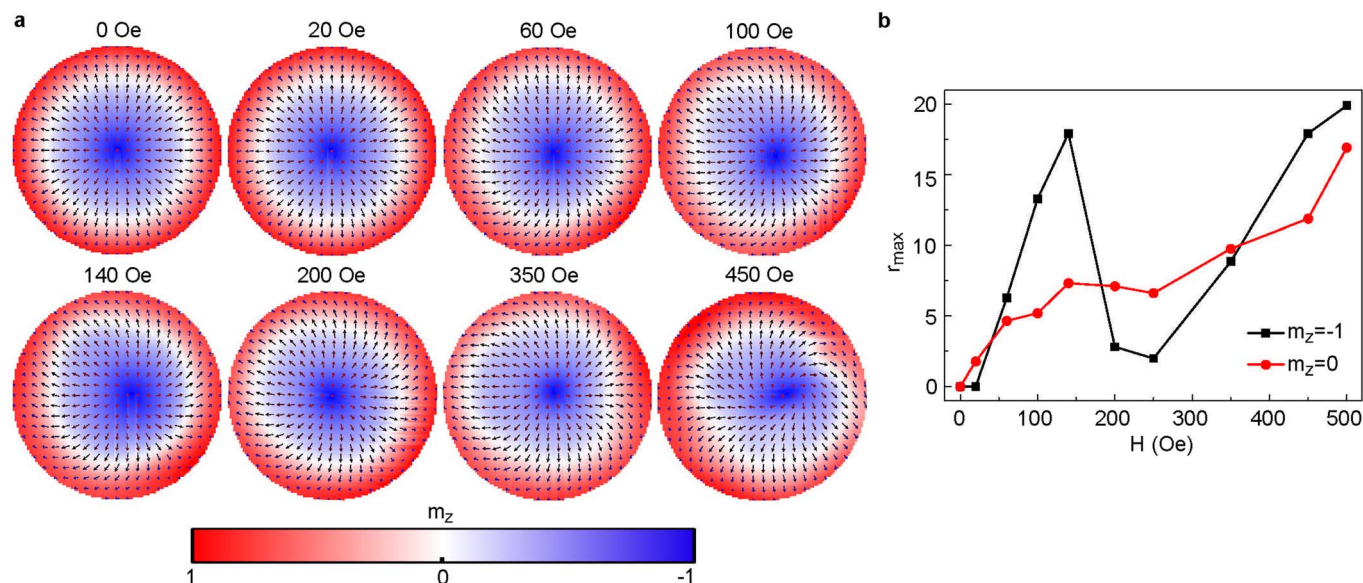


Figure 6 | The magnetization distribution of a skyrmion in a microwave field. The microwave field applied has the same frequency (4.60 GHz) and amplitudes (in the range of 0 ~ 450 Oe) as that in Fig. 4. (a) The corresponding magnetization distribution to the topological density distribution of skyrmion (Fig. 4) under different field amplitude. The colors represent the magnitude of the out-of-plane magnetization component (m_z) and the arrows represent the direction of magnetization projected in the plane at each point. (b) The maximum position displacement r_{max} from the zero-field position as a function of field amplitude for both skyrmion core ($m_z = -1$) and boundary ($m_z = 0$). r_{max} is chosen as follows. The initial position of m_z at a zero magnetic field is r_0 but changes to r_1 in a magnetic field, the maximum value of $|r_1 - r_0|$ is selected for plotting.



spectrum has only one peak which is associated with the driving field. Changing the amplitude from 100 to 200 Oe to intensify the deformation of the topological density distribution leads to the appearance of a flower-like trajectory with an additional FFT peak at 1.10 GHz (Fig. 7b). A larger value of the amplitude seems necessary at 3.45 GHz than at 4.60 GHz to trigger the flower-like trajectory of a skyrmion. These results further confirm that the deformation of the topological density distribution is vital for the stability of mode 1 near 1.15 GHz and hence for the flower-like trajectories. Complementary to the trajectory of the guiding center in Fig. 7a is the trajectory of the average magnetization. Figures 7c and 7d show the corresponding trajectories of the average magnetization of coupled skyrmions in a microwave field with a frequency of 3.45 GHz and amplitudes of 100 and 200 Oe. The three-dimensional (3D) plot of the magnetization shows periodic behavior when the field amplitude is 100 Oe. Its 2D projection on the xy plane is a circle while, when the field amplitude increases to 200 Oe, the 3D plot is complex with knots and shows quasiperiodic behavior. Surprisingly, its 2D projection on the xy plane shows a flower-like trajectory, similar to that of the guiding center (Fig. 7d), which indicates that flower-like dynamics may be observed by detecting the volume-averaged magnetization signal at different times in the experiment.

Figure 8 demonstrates the trajectory of the guiding center when a microwave field is applied to both the top and the bottom nanolayers. The field amplitude is 200 Oe and the frequency 4.6 GHz. Because of the opposite chiralities of the two skyrmions, the two guiding centers move oppositely and separate from each other. If there were no magnetostatic interaction between the two guiding centers, one would expect two independent microwave-field-induced flower-like trajectories in both the top and the bottom nanolayer. However, this center separation will change the interlayer magnetostatic interaction which has an effect opposite to the microwave field and may destroy the flower-like trajectories. This is different from the case previously discussed with the microwave field only applied to one nanolayer, in which the magnetostatic interaction plays a positive role and forces the other nanolayer to a synchronic flower-like trajectory. Though the two guiding centers move oppositely, the

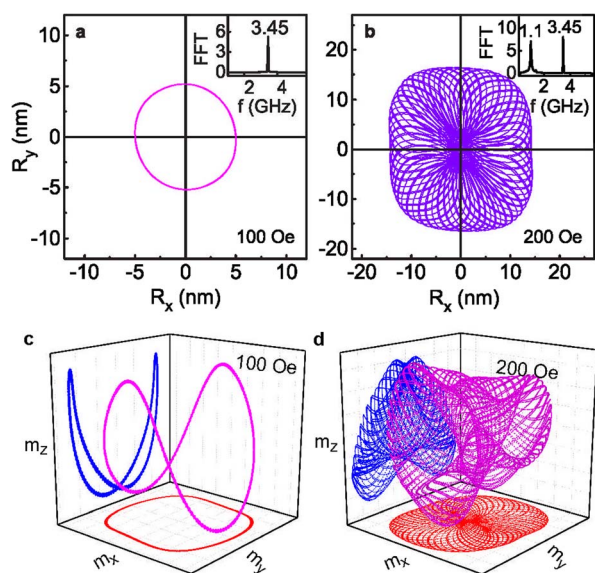


Figure 7 | Influence of the topological density distribution deformation on the dynamics of a skyrmion. The trajectories of the guiding center in 30 ~ 50 ns are shown. The frequency of the microwave field is 3.45 GHz and the amplitude 100 Oe (a) and 200 Oe (b). The insets in the right corners are the corresponding FFT spectra. The corresponding trajectories of the average magnetization of the system in 100 Oe (c) and 200 Oe (d) fields are also given.

initial rotation direction of the two guiding centers is the same (CCW), as shown in the upper-right insets. In addition, the magnetostatic interaction between the two skyrmions is strong, which leads to a smaller distance of motion than that in Fig. 3. It should be noted that the rotation direction of both guiding centers does not change direction (indicated in the lower-right insets), which is different from the results in Figs. 2b and 3.

Discussion

We have observed complex flower-like dynamics with dual resonant modes activated by a single-frequency microwave magnetic field in coupled skyrmions by means of micromagnetic simulations. The occurrence of flower-like dynamics is associated with the large non-local deformation of the topological density distribution of coupled skyrmions. The novel non-linear resonant excitations can be controlled systematically by the amplitude and frequency of the external magnetic field, for example from a circular trajectory to different flower-like ones. Because of its global smooth topological spin texture, a skyrmion can undergo a large non-local deformation of the magnetization distribution by a microwave field or by spin-transfer torque which leads to a global deformation of the topological density distribution. Therefore, we expect that similar flower-like dynamics can also be activated in other skyrmion systems, such as a single skyrmion or a skyrmion crystal stabilized by the DMI^{10,27,28}, not limited to coupled skyrmions, which may lead to observing flower-like dynamics easier in an experiment. These findings contribute to an understanding of complex non-linear dynamics of topological objects and are essential for manipulation of skyrmions in future applications.

Methods

Micromagnetics simulations. Three-dimensional (3D) micromagnetic simulations have been utilized to study the dynamical behavior of coupled skyrmions in Co/Ru/Co nanodisks in an external magnetic field by means of the object oriented micromagnetic framework (OOMMF) code²⁹. For the cobalt material parameters, we used the saturation magnetization $M_s = 1.4 \times 10^6$ A/m, the exchange stiffness $A_{ex} = 3.0 \times 10^{-11}$ J/m, and the uniaxial anisotropy constant $K_u = 5.2 \times 10^5$ J/m³ in the direction perpendicular to the nanodisk plane. The diameter of the Co/Ru/Co nanodisk was chosen to be 200 nm and the thickness of Co and Ru 18 nm and 2 nm, respectively. In the geometry, coupled skyrmions can be formed as a ground state¹⁴. The cell size was $2 \times 2 \times 2$ nm³ and the dimensionless damping α was 0.02. The interfacial coupling coefficient of the adjacent surfaces was -5×10^{-5} J/m². The method of obtaining static coupled skyrmions is the same as that used in Ref. 14: Different initial magnetic states (vortex-like, in-plane-like, and out-of-plane-like initial states) were used to obtain the most stable state. To realize coupled static skyrmions in an experiment, we suggest to saturate the magnetization of the system by applying a magnetic field along +z direction (perpendicular to the disk plane), then reduce the field to zero and, finally, coupled skyrmions can be expected to form.

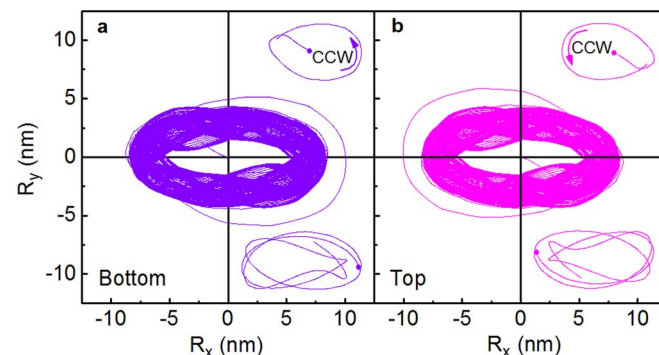


Figure 8 | Trajectories of the guiding center in a magnetic field with amplitude 200 Oe and frequency 4.6 GHz. The magnetic field is applied on both the top and bottom nanolayers. Trajectories of the guiding center in the (a) bottom and (b) top nanolayers. The insets in the upper- and lower-right corners are the initial and steady trajectories, respectively. The starting points are labelled by dots and the arrows indicate the rotation direction of the guiding center.



To investigate the resonant excitations of the coupled skyrmion, an external microwave magnetic field was applied along the $+x$ axis to the top static skyrmion with different frequencies and amplitudes. So far, microwave technologies in nanostructures have achieved great progress, such as realizing spin waves and microwaves propagating in nanostructures via a nanostructured waveguide^{30–32}. In an experiment, we expect that the microwave magnetic field can be precisely applied to the top nanolayer by means of a nanoscale waveguide in future.

1. Skyrme, T. H. R. A unified field theory of mesons and baryons. *Nucl. Phys.* **31**, 556–569 (1962).
2. Okamura, Y. *et al.* Microwave magnetoelectric effect via skyrmion resonance modes in a helimagnetic multiferroic. *Nat. Commun.* **4**, 2391 (2013).
3. Jonietz, F. *et al.* Spin Transfer Torques in MnSi at Ultralow Current Densities. *Science* **330**, 1648–1651 (2010).
4. Lee, M., Kang, W., Onose, Y., Tokura, Y. & Ong, N. P. Unusual Hall Effect Anomaly in MnSi under Pressure. *Phys. Rev. Lett.* **102**, 186601 (2009).
5. Zang, J., Mostovoy, M., Han, J. H. & Nagaosa, N. Dynamics of Skyrmion Crystals in Metallic Thin Films. *Phys. Rev. Lett.* **107**, 136804 (2011).
6. Schulz, T. *et al.* Emergent electrodynamics of skyrmions in a chiral magnet. *Nat. Phys.* **8**, 301–304 (2012).
7. Nagaosa, N. & Tokura, Y. Topological properties and dynamics of magnetic skyrmions. *Nat. Nanotechnol.* **8**, 899–911 (2013).
8. Yu, X. Z. *et al.* Skyrmion flow near room temperature in an ultralow current density. *Nat. Commun.* **3**, 988 (2012).
9. Mühlbauer, S. *et al.* Skyrmion lattice in a chiral magnet. *Science* **323**, 915–919 (2009).
10. Yu, X. Z. *et al.* Real-space observation of a two-dimensional skyrmion crystal. *Nature* **465**, 901–904 (2010).
11. Adams, T. *et al.* Long-Range Crystalline Nature of the Skyrmion Lattice in MnSi. *Phys. Rev. Lett.* **107**, 217206 (2011).
12. Heinze, S. *et al.* Spontaneous atomic-scale magnetic skyrmion lattice in two dimensions. *Nat. Phys.* **7**, 713–718 (2011).
13. Seki, S., Yu, X. Z., Ishiwata, S. & Tokura, Y. Observation of Skyrmions in a Multiferroic Material. *Science* **336**, 198–201 (2012).
14. Dai, Y. Y. *et al.* Skyrmion ground state and gyration of skyrmions in magnetic nanodisks without the Dzyaloshinsky-Moriya interaction. *Phys. Rev. B* **88**, 054403 (2013).
15. Sun, L. *et al.* Creating an Artificial Two-Dimensional Skyrmion Crystal by Nanopatterning. *Phys. Rev. Lett.* **110**, 167201 (2013).
16. Kiselev, N. S., Bogdanov, A. N., Schäfer, R. & Rößler, U. K. Chiral skyrmions in thin magnetic films: new objects for magnetic storage technologies? *J. Phys. D: Appl. Phys.* **44**, 392001 (2011).
17. Kiselev, S. I. *et al.* Microwave oscillations of a nanomagnet driven by a spin-polarized current. *Nature* **425**, 380–383 (2003).
18. Kong, L. & Zang, J. Dynamics of an Insulating Skyrmion under a Temperature Gradient. *Phys. Rev. Lett.* **111**, 067203 (2013).
19. Lin, S.-Z., Batista, C. D., Reichhardt, C. & Saxena, A. AC current generation in chiral magnetic insulators and skyrmion motion induced by the spin Seebeck effect. Preprint at <http://arxiv.org/abs/1308.2634> (2013).
20. Mochizuki, M. Spin-Wave Modes and Their Intense Excitation Effects in Skyrmion Crystals. *Phys. Rev. Lett.* **108**, 017601 (2012).
21. Petit-Watlot, S. *et al.* Commensurability and chaos in magnetic vortex oscillations. *Nat. Phys.* **8**, 682–687 (2012).
22. Kammerer, M. *et al.* Magnetic vortex core reversal by excitation of spin waves. *Nat. Commun.* **2**, 279 (2011).
23. Makhfudz, I., Krüger, B. & Tchernyshyov, O. Inertia and Chiral Edge Modes of a Skyrmion Magnetic Bubble. *Phys. Rev. Lett.* **109**, 217201 (2012).
24. Moutafis, C., Komineas, S. & Bland, J. A. C. Dynamics and switching processes for magnetic bubbles in nanoelements. *Phys. Rev. B* **79**, 224429 (2009).
25. Papanicolaou, N. & Tomaras, T. N. Dynamics of magnetic vortices. *Nucl. Phys. B* **360**, 425–462 (1991).
26. Wang, H., Dai, Y. Y., Yang, T., Ren, W. J. & Zhang, Z. D. Microwave-driven Topological Resonant Excitations of Coupled Skyrmions. Preprint at <http://arxiv.org/abs/1401.0373> (2014).
27. Yu, X. Z. *et al.* Near room-temperature formation of a skyrmion crystal in thin-films of the helimagnet FeGe. *Nat. Mater.* **10**, 106–109 (2011).
28. Sampaio, J., Cros, V., Rohart, S., Thiaville, A. & Fert, A. Nucleation, stability and current-induced motion of isolated magnetic skyrmions in nanostructures. *Nat. Nanotechnol.* **8**, 839–844 (2013).
29. Donahue, M. J. & Porter, D. G. *OOMMF User's guide, Version 1.0, Interagency Report NISTIR 6376* (Gaithersburg, MD, 1999).
30. Tripon-Canseliet, C. & Chazelas, J. *Nanoscale Microwave Engineering: Optical Control of Nanodevices*. (John Wiley & Sons, 2014).
31. Wang, C.-J. & Lin, L. Y. Nanoscale waveguiding methods. *Nanoscale Res. Lett.* **2**, 219–229 (2007).
32. Demidov, V. E., Urazhdin, S. & Demokritov, S. O. Control of spin-wave phase and wavelength by electric current on the microscopic scale. *Appl. Phys. Lett.* **95**, 262509 (2009).

Acknowledgments

We thank Prof. Frank R de Boer for the helpful discussions. The work is supported by the National Basic Research Program (No. 2010CB934603) of China, Ministry of Science and Technology China and the National Natural Science Foundation of China under Grant No. 51331006.

Author contributions

Y.Y.D. and H.W. carried out the micromagnetic simulations. Y.Y.D., H.W., T.Y. and W.J.R. analyzed and interpreted the data. Y.Y.D. and H.W. wrote the paper. Z.D.Z. proposed this study. All authors discussed the data and contributed to preparing the paper.

Additional information

Supplementary information accompanies this paper at <http://www.nature.com/scientificreports>

Competing financial interests: The authors declare no competing financial interests.

How to cite this article: Dai, Y., Wang, H., Yang, T., Ren, W. & Zhang, Z. Flower-like dynamics of coupled Skyrmions with dual resonant modes by a single-frequency microwave magnetic field. *Sci. Rep.* **4**, 6153; DOI:10.1038/srep06153 (2014).



This work is licensed under a Creative Commons Attribution-NonCommercial-NoDerivs 4.0 International License. The images or other third party material in this article are included in the article's Creative Commons license, unless indicated otherwise in the credit line; if the material is not included under the Creative Commons license, users will need to obtain permission from the license holder in order to reproduce the material. To view a copy of this license, visit <http://creativecommons.org/licenses/by-nc-nd/4.0/>